Unidirectional Pumping of Phonons by Magnetization Dynamics: Supplemental Material

Xiang Zhang,[1] Gerrit E. W. Bauer,[2,1] and Tao Yu[3,1,*]

[1] *Kavli Institute of NanoScience, Delft University of Technology, 2628 CJ Delft, The Netherlands*

[2] *Institute for Materials Research & WPI-AIMR & CSRN, Tohoku University, Sendai 980-8577, Japan*

[3] *Max Planck Institute for the Structure and Dynamics of Matter, 22761 Hamburg, Germany*

(Dated: July 23, 2020)

I. MAGNON AND PHONON MODES

Here we derive the normalized magnetic and mechanical eigenmodes used in the main text.

The Landau-Lifshitz equation for the transverse dynamics in our configuration with saturated magnetization along the $\hat{\mathbf{x}}$ direction reads

$$\begin{aligned}\frac{dm_y}{dt} &= -\mu_0\gamma(H_{\rm app} - N_{xx}M_s + N_{zz}M_s)m_z,\\ \frac{dm_z}{dt} &= \mu_0\gamma(H_{\rm app} - N_{xx}M_s)m_y,\end{aligned} \tag{S1}$$

which is solved by

$$m_z = i\xi_{\rm M}^2 m_y, \tag{S2}$$

with dimensionless ellipticity

$$\xi_{\rm M} = \left(\frac{H_0 - N_{xx}M_s}{H_0 - N_{xx}M_s + N_{zz}M_s}\right)^{1/4}. \tag{S3}$$

When H_0 is large, $\xi_{\rm M} \to 1$. With normalization condition [1, 2]

$$\int d\mathbf{r}\left(m_y m_z^* - m_y^* m_z\right) = -\frac{i}{2}, \tag{S4}$$

the magnon amplitudes read

$$m_y = -\frac{1}{2\sqrt{Lwd}}\frac{1}{\xi_M}, \quad m_z = -\frac{i}{2\sqrt{Lwd}}\xi_M. \tag{S5}$$

We treat the thin YIG nanowire as a small perturbation of the elastic GGG substrate. The surface strains obey the equation of motion [3, 4]

$$\rho\frac{\partial^2 u_i}{\partial t^2} = \sum_j \frac{\partial \sigma_{ij}}{\partial x_j}, \tag{S6}$$

with free boundary condition $\sigma_{ij}|_S = 0$ at the surface "S". We focus on an isotropic material in the linear regime of Hooke's Law $\sigma_{ij} = \sum_{kl} C_{ijkl}\epsilon_{kl}$ with stiffness coefficient C_{ijkl} and strain tensor $\epsilon_{ij} = (\partial u_i/\partial x_j + \partial u_j/\partial x_i)/2$ [3]. The displacement field can be written in terms of the elastic scalar and vector potentials V and $\mathbf{A}$ as $\boldsymbol{u} = \nabla V + \nabla \times \mathbf{A}$, with $\mathbf{A} = A\vec{y}$ because the displacement field of an acoustic wave propagating in the $\vec{x}$ direction does not depend on y. With $u_x = \partial V/\partial x - \partial A/\partial z$ and $u_z = \partial V/\partial z + \partial A/\partial x$ we arrive at

$$\begin{aligned}\frac{\partial^2 V}{\partial x^2} + \frac{\partial^2 V}{\partial z^2} &= \frac{\rho}{\lambda + 2\mu}\frac{\partial^2 V}{\partial t^2},\\ \frac{\partial^2 A}{\partial x^2} + \frac{\partial^2 A}{\partial z^2} &= \frac{\rho}{\mu}\frac{\partial^2 A}{\partial t^2}.\end{aligned} \tag{S7}$$

A sufficiently thin YIG nanowire follows the displacement field of the substrate. By a plane wave ansatz for V and $\mathbf{A}$, we obtain the (unnormalized) amplitudes of the Rayleigh surface acoustic waves (SAWs)

$$\begin{aligned}\psi_x &= ik\varphi_k\left(e^{qz} - \frac{2qs}{k^2+s^2}e^{sz}\right)e^{ikx},\\ \psi_z &= q\varphi_k\left(e^{qz} - \frac{2k^2}{k^2+s^2}e^{sz}\right)e^{ikx},\end{aligned} \tag{S8}$$

where $q = \sqrt{k^2 - k_l^2}$ and $s = \sqrt{k^2 - k_t^2}$ have been introduced in the main text. The surface modes decay exponentially on two lengths as e^{qz} and e^{sz} and a single node. We normalize the SAW as [5]

$$\int_{-\infty}^{0} dz \left(|\psi_x|^2 + |\psi_z|^2\right) = \frac{\hbar}{2\rho L \omega_k}, \tag{S9}$$

leading to the normalization factor

$$\varphi_k = \frac{1}{|k|} \frac{1+b^2}{2a(1-b^2)} \sqrt{\frac{2\hbar}{\rho L c_r}}\, \xi_P, \tag{S10}$$

where

$$\xi_{\mathrm{P}} = \frac{a(1-b^2)}{1+b^2} \left(\frac{1+a^2}{2a} + \frac{2a(a-2b)}{b(1+b^2)} \right)^{-1/2} \tag{S11}$$

with dimensionless material constants

$$\begin{aligned} a &= q/|k| = \sqrt{1-(c_r/c_l)^2}, \\ b &= s/|k| = \sqrt{1-\eta^2}. \end{aligned} \tag{S12}$$

Here $c_r = \eta\sqrt{\mu/\rho}$ and $c_l = \sqrt{(\lambda+2\mu)/\rho}$ are the sound velocities of the surface and longitudinal bulk waves, respectively.

The node in the eigenmodes leads to zeros in the z-dependence of the excited phonon spin density (parameters in the main text), as shown in Fig. S1 for typical parameters.

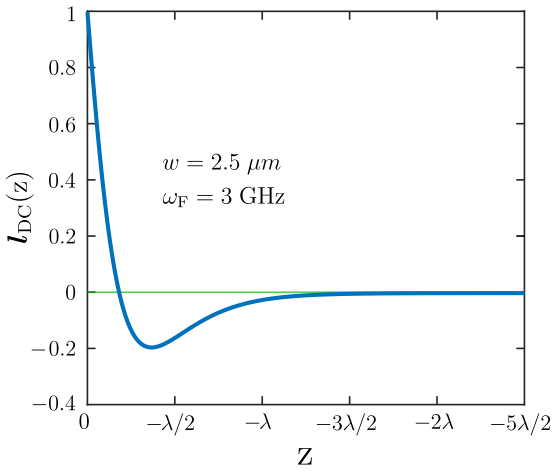

FIG. S1. (Color online) Depth (z) dependence of the excited phonon spin density, normalized by the surface amplitude ($z = 0$) (for the parameters in the main text).

II. CLASSICAL FORMALISM OF SAWS PUMPING

Here we formulate the excitation of Rayleigh SAWs by the oscillating surface force

$$\boldsymbol{F}|_{x=\pm\frac{w}{2}+x_i} = \frac{\delta H_c}{\delta u_z(x,t)} = \mp \frac{B_\perp L d}{M_s} M_z \vec{z}, \tag{S13}$$

that arises from the magnetoelastic coupling [4, 6], which is consistent with the matrix elements in the (quantum) Hamiltonian approach used in the text.

The boundary conditions for the stress tensor (line load)

$$\begin{aligned}\sigma_{zz}|_{z=0_-} &= \frac{1}{L}\frac{dF(x,z)}{dx} \simeq -\frac{B_\perp d}{M_s}\hat{M}_z\left[\delta\left(x-\left(\frac{w}{2}+x_i\right)\right)-\delta\left(x-\left(-\frac{w}{2}+x_i\right)\right)\right],\\ \sigma_{xz}|_{z=0_-} &= 0,\end{aligned} \tag{S14}$$

conserve momentum [4, 6]. We solve the elastic equation of motion [Eq. (S7)] with these conditions by a plane-wave ansatz (dropping the explicit time harmonic) [4]

$$\begin{aligned}V &= \int_{-\infty}^{\infty}\mathcal{V}(k)e^{i\left(kx+\sqrt{k_l^2-k^2}z\right)}dk,\\ A &= \int_{-\infty}^{\infty}\mathcal{A}(k)e^{i\left(kx+\sqrt{k_t^2-k^2}z\right)}dk.\end{aligned} \tag{S15}$$

The Fourier transform of the boundary condition $\sigma_{zz}(k)|_{z=0} = if_z/(\mu\pi)\sin(kw/2)e^{-ikx_i}$ with $f_z = (B_\perp d/M_s)\hat{M}_z$ and $\sigma_{xz}(k)|_{z=0} = 0$ leads to dynamic elastic potentials in k-space

$$\begin{aligned}\mathcal{V}(k) &= i\frac{f_z}{\pi\mu}\frac{2k^2-k_t^2}{F(k)}\sin\left(\frac{kw}{2}\right)e^{-ikx_i},\\ \mathcal{A}(k) &= -\frac{f_z}{\pi\mu}\frac{2k\sqrt{k^2-k_l^2}}{F(k)}\sin\left(\frac{kw}{2}\right)e^{-ikx_i},\end{aligned} \tag{S16}$$

with

$$F(k) = (2k^2-k_t^2)^2 - 4k^2\sqrt{k^2-k_l^2}\sqrt{k^2-k_t^2}. \tag{S17}$$

$F(k) = 0$ is the so-called Rayleigh equation. The displacement field at the substrate surface ($z = 0$)

$$\begin{aligned}u_x|_{z=0} &= -\frac{f_z}{\pi\mu}\int_{-\infty}^{\infty}\frac{k\sin(kw/2)}{F(k)}\left[(2k^2-k_t^2)-2\sqrt{k^2-k_l^2}\sqrt{k^2-k_t^2}\right]e^{ik(x-x_i)}\,dk,\\ u_z|_{z=0} &= -\frac{if_zk_t^2}{\pi\mu}\int_{-\infty}^{\infty}\frac{\sqrt{k^2-k_l^2}\sin(kw/2)}{F(k)}e^{ik(x-x_i)}\,dk.\end{aligned} \tag{S18}$$

Far from the nanowire $|x| > x_i$, the integrals can be carried out analytically by following the contours in Fig. S2. The roots of the Rayleigh equation $F(k_r) = 0$ are poles, while $\pm k_l$ and $\pm k_t$ are branch cuts. We can carry out the contour integral by closing the contours depending on $x > x_i$ or $x < x_i$. Using Watson's lemma for the asymptotic treatment of the integral along the branch cuts the displacement field on the substrate surface ($z = 0$) reads

$$\begin{aligned}u_x^\pm|_{z=0} &= \pm\frac{if_z}{2\mu}\frac{(1-b^2)}{-4+(1+b^2)\left[1+\frac{1}{2}\left(\frac{1}{a^2}+\frac{1}{b^2}\right)\right]}\sin\left(\frac{k_rw}{2}\right)e^{\pm ik_r(x-x_i)}\\ &\pm\frac{2f_ze^{-i\frac{\pi}{4}}}{\mu}\sqrt{\frac{2}{\pi}}\sqrt{\frac{a^2-b^2}{1-b^2}}\left(\frac{(1-a^2)^{\frac{1}{2}}(1-b^2)^{\frac{3}{2}}}{(1+b^2-2a^2)^3}\sin\left(\frac{k_lw}{2}\right)\frac{e^{\pm ik_l(x-x_i)}}{[k_l(x-x_i)]^{3/2}}+\sin\left(\frac{k_tw}{2}\right)\frac{e^{\pm ik_t(x-x_i)}}{[k_t(x-x_i)]^{3/2}}\right)\\ &+\mathcal{O}(kx)^{-\frac{5}{2}},\end{aligned} \tag{S19}$$

$$\begin{aligned}u_z^\pm|_{z=0} &= -\frac{f_z}{\mu}\frac{a(1-b^2)}{(1+b^2)\left[-4+(1+b^2)[1+\frac{1}{2}(\frac{1}{a^2}+\frac{1}{b^2})]\right]}\sin\left(\frac{k_rw}{2}\right)e^{\pm ik_r(x-x_i)}\\ &+\frac{f_ze^{i\frac{\pi}{4}}}{\mu}\sqrt{\frac{2}{\pi}}\left(\frac{(1-a^2)(1-b^2)}{(1+b^2-2a^2)^2}\sin\left(\frac{k_lw}{2}\right)\frac{e^{\pm ik_l(x-x_i)}}{[k_l(x-x_i)]^{3/2}}+\frac{4(a^2-b^2)}{1-b^2}\sin\left(\frac{k_tw}{2}\right)\frac{e^{\pm ik_t(x-x_i)}}{[k_t(x-x_i)]^{3/2}}\right)\\ &+\mathcal{O}(kx)^{-\frac{5}{2}},\end{aligned} \tag{S20}$$

where the " $\pm$ " sign stands for the right- and left-going waves on the right and left sides of the wire, respectively. The second terms decay far from the nanowire as $1/(k_l x)^{3/2}$ and $1/(k_t x)^{3/2}$ and can be attributed to the evanescent contributions from longitudinal ($e^{ik_l x}$) and transverse ($e^{ik_t x}$) bulk acoustic waves. These contributions can be disregarded far from the nanowire, where only the Rayleigh SAWs ($e^{ik_r x}$) survive.

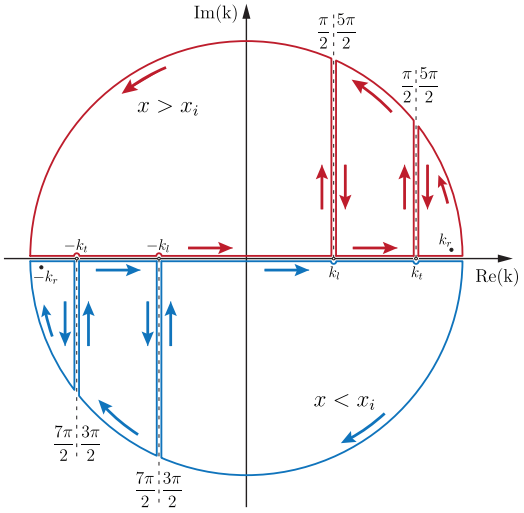

FIG. S2. Contour in the complex k plane. The upper half plane is used when $x > x_i$ and lower half plane when $x < x_i$. Branch cuts at $\pm k_l$ and $\pm k_t$ are indicated. The Rayleigh points $\pm k_r$ acquire a small imaginary part by causality or sound attenuation.

Retaining only the SAWs, we find the displacement field from the integral for general z,

$$\begin{aligned} u_x &= -\frac{f_z}{\pi\mu}\int_{-\infty}^{\infty}\frac{k\sin(kw/2)}{F(k)}\left[(2k^2-k_t^2)\,e^{\sqrt{k^2-k_l^2}z}-2\sqrt{k^2-k_l^2}\sqrt{k^2-k_t^2}\,e^{\sqrt{k^2-k_t^2}z}\right]e^{ik(x-x_i)}\,dk,\\ u_z &= \frac{if_z}{\pi\mu}\int_{-\infty}^{\infty}\frac{\sqrt{k^2-k_l^2}\sin(kw/2)}{F(k)}\left[(2k^2-k_t^2)\,e^{\sqrt{k^2-k_l^2}z}-2k^2\,e^{\sqrt{k^2-k_t^2}z}\right]e^{ik(x-x_i)}\,dk, \end{aligned} \tag{S21}$$

and

$$\begin{aligned} u_x^{\pm} &= \pm\frac{if_z}{\mu}\frac{1}{-4+(1+b^2)\left[1+\frac{1}{2}(\frac{1}{a^2}+\frac{1}{b^2})\right]}\sin\left(\frac{k_r w}{2}\right)\left[e^{qz}-\frac{2ab}{1+b^2}e^{sz}\right]e^{\pm ik_r(x-x_i)},\\ u_z^{\pm} &= \frac{f_z}{\mu}\frac{a}{-4+(1+b^2)\left[1+\frac{1}{2}(\frac{1}{a^2}+\frac{1}{b^2})\right]}\sin\left(\frac{k_r w}{2}\right)\left[e^{qz}-\frac{2}{1+b^2}e^{sz}\right]e^{\pm ik_r(x-x_i)}. \end{aligned} \tag{S22}$$

Inserting the force term $f_z = B_\perp \hat{M}_z/M_s$ and the expression for M_z from the main text, we arrive at the pumped displacement fields,

$$\begin{aligned} u_x^{\pm} &= \mp\frac{B_\perp\xi_M\xi_P}{\rho c_r^2}\sqrt{\frac{2\hbar\gamma d}{LwM_s}}\frac{\xi_P}{1-b^2}\sin\left(\frac{k_r w}{2}\right)\left(e^{qz}-\frac{2ab}{1+b^2}e^{sz}\right)e^{\pm ik_r(x-x_i)}\langle\hat{\beta}(t)\rangle\\ &= -\frac{1}{c_r}i\psi_x g^*_{\pm k_r}\langle\hat{\beta}(t)\rangle,\\ u_z^{\pm} &= \frac{iB_\perp\xi_M\xi_P}{\rho c_r^2}\sqrt{\frac{2\hbar\gamma d}{LwM_s}}\frac{a\xi_P}{1-b^2}\sin\left(\frac{k_r w}{2}\right)\left(e^{qz}-\frac{2}{1+b^2}e^{sz}\right)e^{\pm ik_r(x-x_i)}\langle\hat{\beta}(t)\rangle\\ &= -\frac{1}{c_r}i\psi_z g^*_{\pm k_r}\langle\hat{\beta}(t)\rangle, \end{aligned} \tag{S23}$$

in which we used the Rayleigh relation $4ab = (1+b^2)^2$ [3]. These results agree with those derived in the main text by the quantum formalism.

III. MICROWAVE TRANSMISSION SPECTRA

Here we address the excitation of magnons and phonons for two parallel magnetic nanowires on a dielectric substrate. One wire is excited by a microwave source, while the other is coupled inductively to another stripline. We compute here the microwave scattering matrix. The Kittel-magnon operators for the two magnetic nanowires at R_1 and R_2 are expressed by $\hat{\beta}_L$ and $\hat{\beta}_R$, respectively. Augmented by the magnetic and elastic damping and microwave input $\hat{p}^{\rm L}_{\rm in}$ acting on the left nanowire, the Heisenberg equations of motion for the magnon-phonon coupled system (including source and dissipation) read

$$\begin{aligned}
\frac{d\hat{\beta}_{\rm L}}{dt} &= -i\hbar\omega_{\rm F}\hat{\beta}_{\rm L}(t) - i\hbar\sum_k |g_k| e^{ikR_1}\hat{b}_k(t) - \left(\frac{\kappa_{\rm L}+\kappa_{\omega,{\rm L}}}{2}\right)\hat{\beta}_{\rm L}(t) - \sqrt{\kappa_{\omega,{\rm L}}}\,\hat{p}^{\rm L}_{\rm in}(t),\\
\frac{d\hat{\beta}_{\rm R}}{dt} &= -i\hbar\omega_{\rm F}\hat{\beta}_{\rm R}(t) - i\hbar\sum_k |g_k| e^{ikR_2}\hat{b}_k(t) - \frac{\kappa_{\rm R}}{2}\hat{\beta}_{\rm R}(t),\\
\frac{d\hat{b}_k}{dt} &= -i\hbar\omega_k\hat{b}_k(t) - i\hbar|g_k| e^{-ikR_1}\hat{\beta}_{\rm L}(t) - i\hbar|g_k| e^{-ikR_2}\hat{\beta}_{\rm R}(t) - \frac{\delta_k}{2}\hat{b}_k(t).
\end{aligned} \tag{S24}$$

Here $\kappa_{\rm L}$ and $\kappa_{\rm R}$ denote the (Gilbert) damping of the Kittel modes in the left and right nanowires, and $\kappa_{\omega,{\rm L}}$ is the radiative coupling of the left nanowire to the microwave source. For sufficiently large $|R_2 - R_1|$ (tens of micrometers for the present system), the excited magnon and phonon operators in frequency space read

$$\begin{aligned}
\hat{\beta}_{\rm L}(\omega) &= \frac{-i\sqrt{\kappa_{\omega,{\rm L}}}}{\omega-\omega_{\rm F}+i\frac{\kappa_{\rm L}+\kappa_{\omega,{\rm L}}}{2}-\sum_k |g_k|^2 G_k(\omega) - f(\omega)}\,\hat{p}^{\rm L}_{\rm in}(\omega),\\
\hat{\beta}_{\rm R}(\omega) &= \frac{\sum_k |g_k|^2 G_k(\omega)\, e^{ik(R_2-R_1)}}{\omega-\omega_{\rm F}+i\kappa_{\rm R}/2-\sum_k |g_k|^2 G_k(\omega)}\,\hat{\beta}_{\rm L}(\omega),\\
\hat{b}_k(\omega) &= |g_k| G_k(\omega)\left(e^{-ikR_1}\hat{\beta}_{\rm L}(\omega) + e^{-ikR_2}\hat{\beta}_{\rm R}(\omega)\right),
\end{aligned} \tag{S25}$$

where

$$f(\omega) = \frac{\left(|g_k|^2/c_r\right)^2 e^{i2\omega(R_2-R_1)/c_r}}{\omega-\omega_{\rm F}+i\kappa_{\rm R}/2-\sum_k |g_k|^2 G_k(\omega)}. \tag{S26}$$

The phonon operator $\hat{b}_k$ governs the displacement field in the main text.

The microwave output of the left and right nanowires is inductively detected by striplines represented by photon operators $\hat{p}^L_{\rm out}$ and $\hat{p}^R_{\rm out}$ that are related by the input-output relations [7, 8]

$$\begin{aligned}
\hat{p}^{\rm L}_{\rm out}(\omega) &= \hat{p}^{\rm L}_{\rm in}(\omega) + \sqrt{\kappa_{\omega,{\rm L}}}\,\hat{\beta}_{\rm L}(\omega),\\
\hat{p}^{\rm R}_{\rm out}(\omega) &= \sqrt{\kappa_{\omega,{\rm R}}}\,\hat{\beta}_{\rm R}(\omega).
\end{aligned} \tag{S27}$$

The microwave reflection (S_{11}) and transmission (S_{21}) spectra become

$$\begin{aligned}
S_{11}(\omega) &\equiv \frac{\hat{p}^{\rm L}_{\rm out}}{\hat{p}^{\rm L}_{\rm in}} = 1 - \frac{i\kappa_{\omega,L}}{\omega-\omega_{\rm F}+i(\kappa_L+\kappa_{\omega,L})/2-\sum_k |g_k|^2 G_k(\omega) - f(\omega)},\\
S_{21}(\omega) &\equiv \frac{\hat{p}^{\rm R}_{\rm out}}{\hat{p}^{\rm L}_{\rm in}} = (S_{11}(\omega)-1)\sqrt{\frac{\kappa_{\omega,R}}{\kappa_{\omega,L}}}\,\frac{\sum_k |g_k|^2 G_k(\omega)\, e^{ik(R_2-R_1)}}{\omega-\omega_{\rm F}+i\kappa_R/2-\sum_k |g_k|^2 G_k(\omega)}.
\end{aligned} \tag{S28}$$

When the two magnetic nanowires are identical, the microwave transmission with excitation (input) at R_1 and detection (output) at R_2,

$$S_{21}(\omega) = (S_{11}(\omega)-1)\,\langle\hat{\beta}_{\rm R}(\omega)\rangle/\langle\hat{\beta}_{\rm L}(\omega)\rangle, \tag{S29}$$

can measure the phase relation between the Kittel modes at FMR in the two wires:

$$S_{21}(\omega_{\rm F}) = (1 - S_{11}(\omega_{\rm F}))\,\chi(k_r)e^{ik_r(R_2-R_1)}.$$

Here $\chi(k_r)$ stands for the ratio of the magnetization amplitudes in the right and left nanowires, as defined in the main text. At the special microwave frequencies $\omega_n = \omega_{\rm F} = \pi c_r(n+1/2)/(R_2-R_1)$, where n is a non-negative integer, $S_{11}(\omega_{\rm F})$ is real while the phase factor $e^{ik_r(R_2-R_1)} = i(-1)^n$ becomes purely imaginary and $\mathrm{Re}\, S_{12}(\omega_{\rm F} = \omega_n) = 0$ develops minima. However, the microwave transmission alone cannot detect the chirality of the excited displacement field, which must therefore be found by other means.

We plot the real part of the transmission amplitude in Fig. S3 as a function of microwave frequency close to $\omega_{\rm F} = 3$ GHz and static magnetic field H_0. Here, with $w = 2.5$ μm and thickness $d = 200$ nm for the YIG nanowires, the additional damping coefficient $\alpha = 1.2 \times 10^{-4}$. The intrinsic magnetic damping is chosen as $\kappa_m = 8 \times 10^{-5}\,\omega_{\rm F} = 0.24\,$MHz and the radiative damping $\kappa_\omega = 1$ MHz. The dips in the transmission are traced by the black contour in Fig. S3(a), while the horizontal dash lines correspond to the special frequencies $\omega_n = \pi c_r(n+1/2)/(R_2-R_1)$, where n is a non-negative integer. Due to the magnon-phonon coupling, these horizontal lines are deformed to the anti-crossings when $\omega_{\rm F} \to \omega_n$. Indeed, we can understand these features by $S_{12}(\omega_{\rm F}) \to (1-S_{11}(\omega_{\rm F}))e^{ik_r(R_2-R_1)}$, where $S_{11}(\omega_{\rm F})$ is real while the phase factor $e^{ik_r(R_2-R_1)} = i(-1)^n$ becomes purely imaginary and then $\mathrm{Re}\, S_{12}(\omega_{\rm F} = \omega_n) = 0$. The dips in the transmission on the FMR resonance line are shown in Fig. S3(b). We note that the transmission does not vanish at dips as it becomes purely imaginary. For $R_2 - R_1 = 300$ μm the frequency spacing between these dips $\Delta\omega = \pi c_r/(R_2-R_1) = 34.26$ MHz.

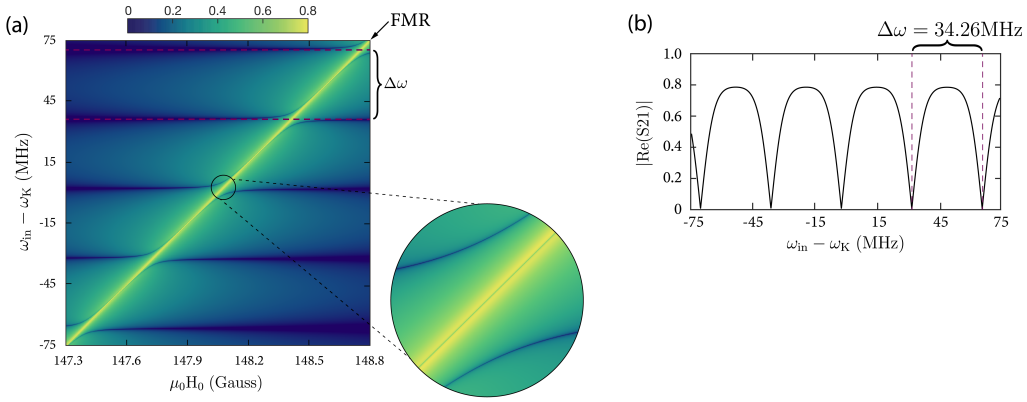

FIG. S3. (Color online) Microwave transmission ($|\mathrm{Re}(S_{21})|$) between two YIG nanowire transducers on top of a GGG substrate. (a) The minima in the transmission (black contour) anticross with the FMR at regularly spaced frequencies ω_n. (b) Transmission spectra at the FMR frequency. The transmission dips originate from the thin black contour hidden within the FMR peaks (yellow region).

* tao.yu@mpsd.mpg.de

[1] L. R. Walker, Phys. Rev. **105**, 390 (1957).

[2] T. Yu, S. Sharma, Y. M. Blanter, and G. E. W. Bauer, Phys. Rev. B **99**, 174402 (2019).

[3] G. S Kino. *Acoustic Waves: Devices, Imaging, And Analog Signal Processing.* (Prentice-Hall, New Jersey, 1987).

[4] I. A. Viktorov. *Rayleigh and Lamb waves: Physical theory and applications.* (Plenum Press, New York, 1967).

[5] M. J. A. Schuetz, E. M. Kessler, G. Giedke, L. M. K. Vandersypen, M. D. Lukin, and J. I. Cirac, Phys. Rev. X **5**, 031031 (2015).

[6] S. Streib, H. Keshtgar, and G. E. W. Bauer, Phys. Rev. Lett. **121**, 027202 (2018).

[7] C. W. Gardiner and M. J. Collett, Phys. Rev. A **31**, 3761 (1985).

[8] A. A. Clerk, M. H. Devoret, S. M. Girvin, F. Marquardt, and R. J. Schoelkopf, Rev. Mod. Phys. **82**, 1155 (2010).